THE EFFECTS OF GAMMA RADIATION ON THERMOLUMINESCENT DOSIMETRY UTILIZING LITHIUM FLUORIDE

A Thesis

Submitted to the Graduate Faculty of the
Louisiana State University and
Agricultural and Mechanical College
in partial fulfillment of the
requirements for the degree of
Master of Science

in

Nuclear Engineering

by
Joseph David Bankston, Jr.
B.S., Louisiana State University, 1967
January, 1969

ACKNOWLEDGEMENT

The author would like to express his appreciation to Dr. R. C. McIlhenny of the Louisiana State University Nuclear Science Center for directing this research and serving as major advisor. His assistance and guidance are truly appreciated.

He also thanks Miss Kay Thomas and Jerry Woods for their help.

TABLE OF CONTENTS

LIST OF TABLES

LIST OF FIGURES

ABSTRACT

A mathematical model to explain the effect of gamma radiation on LiF TLD 100 dosimeters was developed. This model was denoted the scavenger-trap model. The basic premises in the development of the scavenger-trap were:

1. There exists scavenging traps which prevent photon emission;
2. Filled scavenger traps dump electrons at temperatures above 300°C;
3. The number of scavenger traps are limited;
4. Radiative traps may be converted to nonradiative traps by exposure to radiation.

First order kinetics was assumed for filling of the traps. Under these premises the response of the dosimeter is expressed as:

$$S = \varepsilon\left[\frac{K_1\alpha A_o}{K_1 + C_1 - C_3}\left(e^{-C_3R} - e^{-(K_1 + C_1)R}\right)\right.$$

$$+ \frac{K_2\,\beta B_o}{K_2 + C_2 - C_4}\left(e^{-C_4R} - e^{-(K_2 + C_2)R}\right) - E_o e^{-C_5R}\left(1 - e^{-K_3A^*}\right)$$

$$\left. - F_o e^{-C_6R}\left(1 - e^{-K_4B^*}\right)\right]$$

where: $$A^* = \frac{K_1\alpha A_o}{K_1 + C_1 - C_3}\left(e^{-C_3R} - e^{-(K_1 + C_1)R}\right)$$

$$B^* = \frac{K_2\beta B_o}{K_2 + C_2 - C_4}\left(e^{-C_4R} - e^{-(K_2 + C_2)R}\right)$$

Since available data was obtained by integration of A^* and B^*, the model was simplified for comparison. The response expressed by the simplified model is:

$$S = \frac{K_1 A_o}{K_1 + C_1 - C_2} \left(e^{-C_2 R} - e^{-(C_1 + K_1)R}\right) - E_o e^{-C_3 R} \left(1 - e^{-C_4 A^*}\right)$$

By empirical fit of the data the following constants were obtained: $K_1 = 1.0 \times 10^{-5}$; $C_1 = 1.5 \times 10^{-5}$; $C_2 = 2.6 \times 10^{-7}$; $C_3 = 9.0 \times 10^{-6}$; $A_o = 1.43 \times 10^{6}$; $E_o = 4.30 \times 10^{6}$. The model predicted the thermoluminescent response of the dosimeters to within an average error of ±3%. In addition, the model also predicted the shape of the sensitization curve. By taking into account both A^* and B^* the radiation damage vs. dose curve was predicted. No attempt was made to identify the trap types with any known crystal defect.

INTRODUCTION

The interaction of radiative energy with an absorbing medium may lead to the promotion of electrons from their ground state to excited states. The excited electrons may immediately return to their ground state, or, in the case of certain crystalline materials, the electrons may remain in excited metastable states. For certain crystalline materials return of the electrons to the ground state with the emission of photons in the visible spectrum may be induced by heat. This is known as thermoluminescence.

The number of photons emitted depends upon the number of electrons returning to the ground state. In turn, the number of electrons returning to the ground state depends upon the number of metastable electrons; and the number of metastable electrons is initially dependent upon the amount of absorbed energy. Since the quantity of light emitted by the crystal may be quantitatively measured, this leads to the possibility of using the thermoluminescence phenomenon for radiation dosimetry.

In the field of personnel monitoring, photographic film is the currently accepted standard of measurement for accumulated dose. Any new dosimetry device must possess certain advantages over the standard film technique of personnel dosimetry. There are several problems in the use of film as a monitoring device, the more important problems of which are:

1. The fact that the photographic film is energy dependent in its response.

2. The film density may vary from batch to batch depending upon emulsion and strength of the developer.

3. The film badge does not approach a point detector.

4. The film has a limited dosage range.

For these reasons, there is a continuing search for dosimeters to replace the film badge.

Of particular interest in the field of personnel dosimetry is the lithium fluoride thermoluminescent dosimeter. In several respects LiF is an ideal thermoluminescent material; it has nearly flat response for all energies of gamma radiations, a large dynamic range, good reproducibility, a relatively large light output for even small doses of absorbed radiation, and small size. In addition the dosimeter is reusable.

The response of LiF as a thermoluminescent dosimeter has, however, not been accurately modeled. In development of such a model the important experimental observations to be described are the following [1] [7]:

1. Lithium fluoride has a linear dose response to about 10^3 R, then a supralinear region to approximately 2.5×10^4 R. Above this dose the response of the dosimeter decreases, and actually shows reversal.

2. When a 400°C anneal is used following radiation exposure, a loss of response (i.e., radiation-induced damage) is noted after about 10^3 R. This damage is noticeably increased if there are several annealings in the exposure history of the dosimeter.

3. If an annealing temperature of 280°C or less is used, the response of the dosimeter is enhanced.

4. At a 600°C anneal it appears that all of the radiation-induced damage is removed.

Development of a workable model should lead to a better understanding of the thermoluminescent response of LiF to absorbed radiation. It is the intent in this thesis to formulate such a model.

FUNDAMENTAL THEORETICAL CONSIDERATION

Crystal Structure [2] [3]

Since LiF is a crystalline material*, it would be helpful to our understanding to delve into the structure of a crystalline substance. A material is termed crystalline when the atoms or molecules which comprise the material are arranged in an ordered lattice over appreciable distances. A lattice is a regular, periodic arrangement of points in space.

An ideal crystal is composed of atoms arranged on a lattice defined by three fundamental translation vectors $\vec{a}$, $\vec{b}$, $\vec{c}$, such that the atomic arrangement looks the same in every respect when viewed from any point $\vec{r}$ as when viewed from a point $\vec{r}'$:

$$\vec{r}' = \vec{r} + n_1\vec{a} = n_2\vec{b} + n_3\vec{c}, \qquad (1)$$

where n_1, n_2, and n_3 are arbitrary integers. The set of points $\vec{r}'$ specified by (1) for all values of integers defines a lattice. A lattice is a mathematical abstraction: the crystal structure is formed only when a basis of atoms is attached identically to each lattice point. The logical relation is the lattice + basis = crystal structure. The basis of LiF is composed of one lithium atom and one fluorine atom.

The lattice and the translation vectors $\vec{a}$, $\vec{b}$, $\vec{c}$, are said to be primitive if any two points $\vec{r}$, $\vec{r}'$ from which the atomic arrangement

---

*LiF is actually a polycrystalline material in which there exist randomly orientated grains. The grains are sub-regions of the material which are themselves of a crystalline structure.

looks the same always satisfy (1) with a suitable choice of the integers n_1, n_2, n_3. The primitive translation vectors are often used to define the crystal axes $\vec{a}$, $\vec{b}$, $\vec{c}$, although non-primitive crystal axes may be used when they are more convenient or simpler. The crystal axes $\vec{a}$, $\vec{b}$, $\vec{c}$, form three adjacent edges of a parallelpiped, as shown in figure 1.

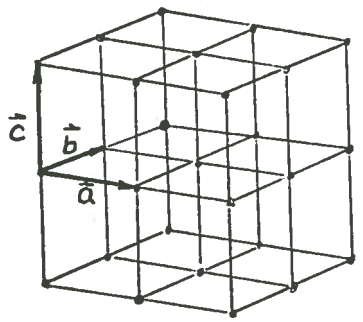

Figure 1. Crystal Structure

If there are lattice points only at the corners of the parallelpiped, then it is a primitive parallelpiped. In a primitive parallelpiped each lattice point is common to eight parallelpipeds. The parallelpiped defined by the primitive axes $\vec{a}$, $\vec{b}$, $\vec{c}$, containing the basis of the crystal is called a unit cell. Thus the unit cells constitute a repetitive, three dimensional structure in space.

In reality the atoms making up the lattice are always slightly displaced by certain vibratory movements, generally of thermal origin. If the movements of the atoms of a lattice are neglected, however, the

electrons are subjected to a field of force depending only on the nuclei. This field has a periodic structure in space. Although this model neglects the interaction of electrons with other electrons (which could cause a nonperiodic structure dependent on time) it is sufficient to explain a great number of phenomena. This hypothesis rests on the idea that electrons in a solid can be classified into two different categories. In the first classification are electrons of the deepest layers of the atom which are only slightly influenced by the presence of other atoms. The second class of electrons are those whose orbitals overlap one another when the atoms are at a normal distance in the lattice. Now, if we consider these peripheral electrons and neglect the repulsions exerted by their neighbors, we see that they lie in a field of forces perfectly periodic in space. Quantum mechanics predicts that the periodic character of the field of force will limit the energies to these values within certain intervals. Between these bands of allowed energy values exist bands of forbidden energy values. The particular bands which are of interest in this study are the conduction band and the valence band, shown schematically in figure 2.

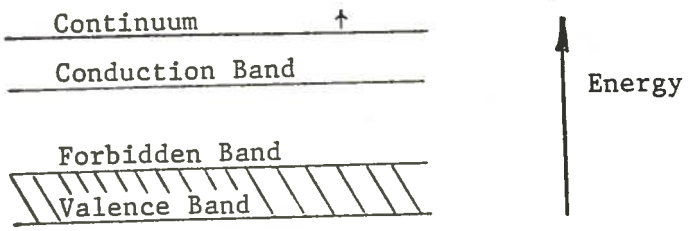

Figure 2. Energy Bands in a Crystal

For an insulator, such as LiF, the valence band contains virtually all of the valence (i.e., peripheral) electrons under ordinary circumstances. Those electrons which have been promoted across the forbidden band (2 to 3 e.v. for LiF) leave vancancies (i.e., holes) in the valence band. Migration of the holes in the valence band and electrons in the conduction band accounts for the very small conductivity of such materials as LiF. Above the top of the conduction band is a continuum of nonquantized states corresponding to the ionized states of single atoms; hence, the top of the conduction band is essentially the "ionization potential" of a true crystal.

It has been observed that the thermoluminescence phenomenon is dependent upon defects in the crystal. That is, in perfect crystals there is no observable luminescence upon heating the crystal, whereas in a crystal with a "large" number of defects we have a readily observable thermoluminescent effect. Therefore, it is of interest to examine lattice defects in crystals. Strictly speaking, a defect is any deviation from a strict periodic crystalline structure; however, we are mainly concerned with dislocations, Schottky and Frenkel defects, and their derivatives.

Most of our knowledge concerning dislocations derives from the interest in metallurgy in the slip process. The experimental and theoretical values of stress required to cause slipping of parallel planes did not coincide. Taylor, Orwan, and Polanyi developed the concept of dislocations to explain this deviation. A dislocation is a series of point vacancies which constitute a continuous plane, as shown

in figure 3. The important aspect of dislocations is that it acts as a series of vacancies for the thermoluminescence phenomena.

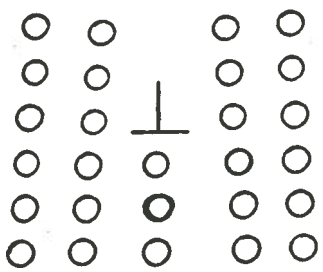

Figure 3. A Dislocation Defect

LiF is an ionic crystal. In an ionic crystal the valence electrons of the metal (lithium) spends most of its time in the vicinity of the halogen (fluorine). Thus an anion-cation pair is created, but the periodicity in space is still maintained.

The simplest imperfection is a lattice vacancy, which is a missing atom or ion, known as a Schottky defect. A Schottky defect in a perfect crystal is formed by transferring an atom from a lattice site in the interior to a lattice site on the surface of the crystal (figure 4).

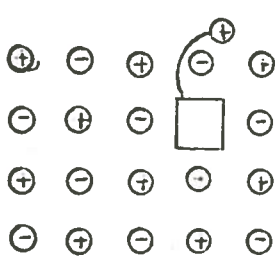

Figure 4. A Defect of Schottky

For thermal equilibrium in an otherwise perfect crystal, a certain number of lattice vacancies are always present because the entropy is increased by the presence of disorder in the structure. At a finite temperature the equilibrium condition of a crystal is the condition of minimum free energy, which means that the equilibrium concentration of vacancies increases with increasing temperature. It is of interest to note that the actual concentration of vacancies will be higher than the equilibrium value if the crystal is raised to a higher temperature and then suddenly cooled, which has the effect of freezing in the vacancies by greatly inhibiting the diffusion of the vacancies in the crystal. In ionic crystals it is usually favorable, from an energy point of view, to form roughly equal numbers of positive and negative ion vacancies. The formation of such pairs of vacancies also have the effect of keeping the crystal electrically neutral on a localized level.

Another type of vacancy defect is the Frenkel defect. In the Frenkel defect, an atom has been displaced from its lattice position to an interstitial position in the crystal, as illustrated in figure 5.

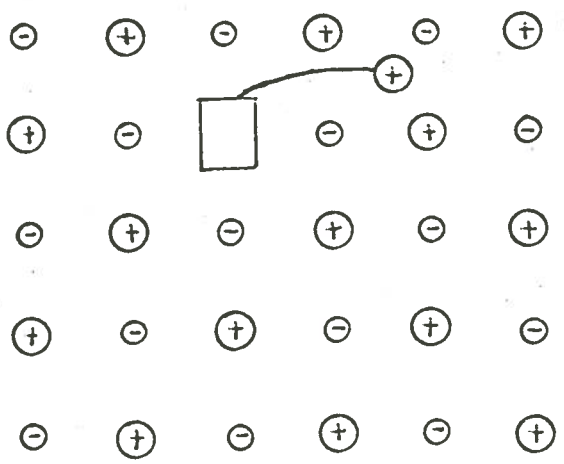

Figure 5. A Frenkel Defect

A negative ion vacancy + interstitial pair is also termed a Frenkel defect. It is of interest to mention that an ion vacancy creates a localized field analogous to a charge of the opposite sign. This vacancy behaves much as a "hydrogen" atom, with discrete levels of energy and a system of wave functions surrounding the vacancy.

A color center is a lattice defect which absorbs visible light. Since an ordinary lattice vacancy does not color alkali halide crystals, there must be another form of defect. A color center may be created in several ways: by the introduction of chemical impurities, or introduction of an excess of metal ion; by x-ray, gamma ray, neutron and electron bombardment; and by electrolysis.

The simplest color center is an F center, which is a negative-ion vacancy in which an electron is trapped. (A negative ion vacancy in a periodic lattice has much the same effect as a positive charge). The distribution of the excess electron is largely on the positive ions (see figure 6). The model which has been adopted for the F center is

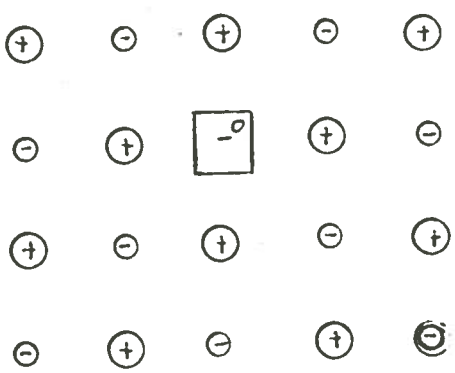

Figure 6. An F Center

consistent with the experimental facts as follows:

1. The F band optical absorption is characteristic of the crystal and not of the method used to produce the F center.

2. Colored crystals are less dense than uncolored crystals. This is in agreement with the idea that the inclusion of vacancies should lower the density of the crystal.

If a crystal containing F center is irradiated, another center, the F_1 center, may be formed. The F_1 center is the association of an F center with an additional electron. This effect is reversible; indeed, it is only appreciable at low temperatures.

If the irradiation of the crystal is carried out at normal temperature, we have the appearance of several absorption bands associated with centers denoted as the R_1, R_2, and M centers. The R_1 center is the association of an F center and a negative ion vacancy; the R_2 center, an association of two F centers; and the M center is the association of an F center with two vacancies of opposite sign. In addition to the above color centers, there are still more complex associations, the coagulation of F centers. This coagulation of F centers is not reversible.

Color centers may also be formed by trapped holes. The best known trapped hole center is the V_1 center in which a positive ion vacancy has trapped a hole. The V_1 center is almost never observed alone but usually in conjunction with V_2, V_3, and V_4 centers, or others. The V_2 center is the association of two V_1 centers, the V_3 the association of a V_1 center and a positive ion vacancy, and the V_4 the association of a V_1 vacancy with two vacancies of the opposite sign. See figure 7 for a summary of the enumerated color centers.

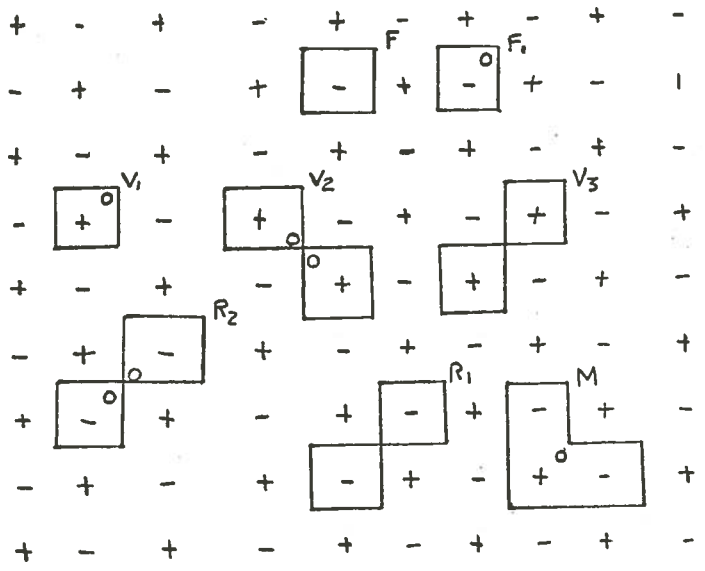

Figure 7. Several Types of Color Centers

The above mentioned defects are intended only as a list of the most common defects, and does not purport to be a complete listing. In addition, it is acknowledged that each type of lattice has its own forms of defects.

In accition to vacancy-associated defects, we may also have impurity defects. In an ionic crystal an impurity atom exists in the state of ions either in an interstitial position or in a site normally occupied by the ion of the crystal. These foreign atoms, because of the difference in their quantum states from the normal atom, they all disturb the periodic quantum states from the normal atom, set up disturbances in the wave functions of the crystals.

In summary, all of the defects have one aspect in common, they all disturb the periodic quantum states of a perfect lattice arrangement. This leads to the possibility of the formation of traps for the electron.

Energy Migration in Crystals [3]

Thermoluminescence involves excited or energetic electron energy states. The migration, or dispersion, of this energy is discussed below.

Consider an electron with energy E_e greater that the ionization energy E_i. This electron is located in a continuum of energy states, and is free to move throughout the crystal in nonquantized states.

Electrons with greater than or equal to the lowest value of the conduction band E_{LC} and less than the ionization energy E_i are located in the conduction band. These electrons are free to move more throughout the crystal but must remain in quantized states in the conduction band.

Considering the electrostatic repulsion between electrons and the attraction between electrons and hole, we must concede the possibility of an association of an electron and hole to form a sort of "hydrogen" atom, called an exciton. The stable states of the exciton are characterized by certain quantized values of energy. The maximum value of this energy, known as exciton ionization, occurs when the electron is located in the conduction band. The minimum value occurs when there is electron-hole recombination, in which case the electron is in the valence band. Thus the exciton energy states are between the conduction band (maximum value) and the valence band (minimum value). This means that the exciton states are in the so-called forbidden zone. (See figure 8.) According to theory, the exciton may move in a lattice; it

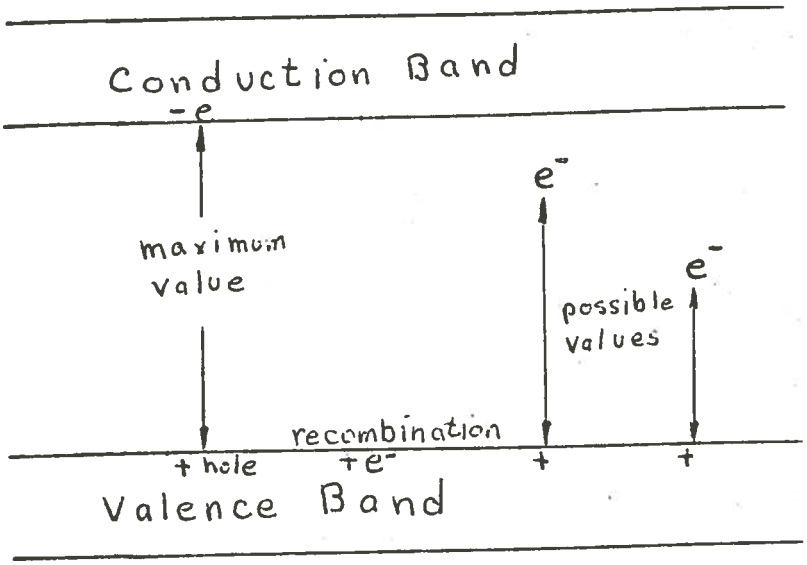

Figure 8. Exciton States

is essentially an energy carrier and does not contribute to current conduction since its effective net charge is zero.

In addition to energy transfer in the movement of electrons and excitons, energy may be transferred by the movement of a neutral atom. This movement is in a quantized manner and is termed tunneling.

Energy may also be distributed in the crystal by photons or phonons. If we have an electron de-excitation by a sudden jump (e.g., the transition from the conduction band to the valence band) there is the production of a photon of energy $E = h\nu$. The momentum of the photon is expressed as $\frac{h\nu}{c}$, where c is the speed of light, h is Plank's constant, and ν is the frequency. However, if we have de-excitation by coupled lattice vibration there will be the emission of a phonon of energy $E = h\nu$. A phonon may be termed a sort of non-

relativistic photon. Its momentum is expressed as $p = \frac{h\nu}{u}$, where u is the speed of the elastic wave. Since u is very much less than c, for photons and phonons of the same energy the phonon has much greater momentum than the photon.

Energy Absorption [4] [3] [5]

In order for an electron to reach a higher energy there must be an input of energy. Since this thesis is concerned with an input of gamma radiation energy, it will be necessary to discuss the possible gamma interactions with matter. Of the several ways in which a gamma ray may lose energy to an absorbing medium, the three most common are the photoelectric effect, Compton scatter, and pair production. In the photoelectric effect the gamma ray interacts with an orbital electron in such a way that essentially all of the energy of the gamma ray is imparted to the electron. As a result of the transfer of energy, the electron is expelled from the atom with a kinetic energy

$$E_e = E_\gamma - B$$

where E_γ is the energy of the gamma ray and B is the binding energy of the electron. Obviously the photoelectric effect requires a gamma ray of greater energy than the binding energy of the electron. Following the expulsion of the electron from the atom, another electron from an outer orbit takes its place in the atom. This transition is accompanied by the emission of x-rays corresponding to the energy difference between the two levels.

The extent of the photoelectric effect is a function of the energy of the gamma radiation and of the atomic number of the absorbing material. The relationship may now be expressed as follows:

$$\text{Probability} = \frac{KZ^n}{E_\gamma^3}$$

where n varies from 3 (for low energy gammas) to 5 (for high energy gamma rays), and K is a constant. (In actual practice, it has been found that the photoelectric effect is important only for gammas of less than one Mev, and then only for high Z absorbers).

In a Compton interaction, a gamma ray photon makes an elastic or "billiard ball" collision with an electron of the absorbing medium. In the collision both energy and momentum are conserved. The relationship between the energy E_γ of the incident photon and the energy E'_γ of the scattered photon and the scattering angle Θ is given by:

$$E'_\gamma = \frac{0.51}{1 - \cos \Theta + 0.51/E_\gamma}$$

Since the Compton effect is an interaction between an orbital electron and a gamma photon, the probability of interaction is dependent upon the number of orbital electrons in the absorber and upon the energy of the incoming gamma photon. A rough approximation of the atomic number energy relationship to the probability of interaction is expressed as:

$$\text{Probability} = \frac{KZ}{E_\gamma},$$

where K is a constant, Z is the atomic number of the absorber and E_γ is the energy of the incoming gamma. A significant difference between the photoelectric effect and Compton scatter is that the former is a true absorption process, whereas for the latter the gamma ray is not absorbed completely. Ultimately, the scattered gamma ray from the Compton scatter will be absorbed as a result of the photoelectric interaction (increasingly probable as the gamma ray energy decreases).

The third interaction is pair production which occurs when a gamma ray with energy in excess of 1.02 Mev passes near the nucleus. When this happens, the photon may be annihilated in the strong electrical field of the nucleus and an electron-positron pair formed. Any excess energy over 1.02 Mev appears mainly as kinetic energy of the electron-positron pair, with a small part of the excess energy being transferred to the nucleus. The probability of pair production is:

$$\text{Probability} = KZ^2 (E-1.02)$$

For an absorber of low Z number, such as LiF, and a gamma-ray energy of 1.25 Mev (average energy of Co^{60}) the principle mode of gamma attenuation is Compton scatter. (See figure 9). In fact, over

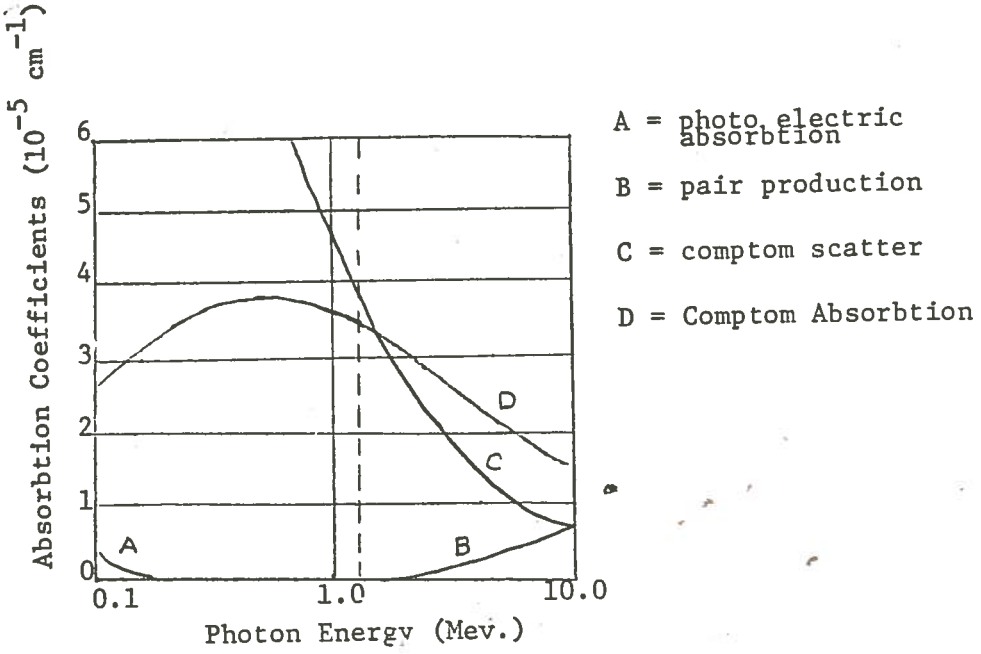

Figure 9. Gamma Ray Absorption Coefficients

99% of the primary interactions are Compton scatter. The average energy of an electron after Compton interaction with 1.25 Mev gamma

may be determined from the relationships found in The Atomic Nucleus by Evans. The necessary relationships are as follows:

(1) $\frac{T_{av}}{h\nu}$ (average kinetic energy of electron = $e^{\sigma a}/e^{\sigma}$

(2) $\sigma a = NZ_e\sigma a$

(3) $\sigma s = e^{\sigma}sNZ$

(4) $\sigma_1 = \sigma_2 \frac{P_1}{P_2} \frac{A_2}{A_1} \frac{Z_1}{Z_2}$

(5) $e^{\sigma} = e^{\sigma}a + e^{\sigma}s$

(6) σa (aluminum) = 0.069 σs (aluminum) = 0.078

let aluminum be denoted as 2 therefore $\sigma_{a2} = 0.069$

$\sigma_{s2} = 0.078$

let σ_{a1} be for either Li or F then $\sigma_{a1} = 0.069 \frac{P_1}{P_2} \frac{A_2}{A_1} \frac{Z_1}{Z_2}$

$\sigma_{s1} = 0.078 \frac{P_1}{P_2} \frac{A_2}{A_1} \frac{Z_1}{Z_2}$

now $\sigma_a = NZe\sigma_a$ therefore $e^{\sigma}s = \frac{\sigma s}{NZ}$

$\sigma_s = NZ_e\sigma_s$ therefore $e^{\sigma}s = \frac{\sigma s}{NZ}$

$e^{\sigma}a1 = 0.069 \frac{P_1}{P_2} \frac{A_2}{A_1} \frac{Z_1}{Z_2} \frac{1}{NZ_1}$

$e^{\sigma}s1 = 0.078 \frac{P_1}{P_2} \frac{A_2}{A_1} \frac{Z_1}{Z_2} \frac{1}{NZ_2}$

now $\frac{T_{av}}{h\nu} = \frac{e^{\sigma}a1}{e^{\sigma}s1 + e^{\sigma}a1}$

$$\frac{T_{av}}{h\nu} = .069 \frac{P_1}{P_2} \frac{A_2}{A_1} \frac{Z_1}{Z_2} \frac{1}{NZ_1}$$

$$0.078 + 0.069 = \frac{P_1}{P_2} \frac{A_2}{A_1} \frac{Z_1}{Z_2} \frac{1}{NZ_1} = \frac{0.069}{0.069 + 0.078} = 0.47$$

since $h\nu(av) = 1.25$ Mev

$$T_{av} = (1.25)(0.47) \text{ Mev} = 0.59 \text{ Mev}$$

The average energy of an electron after the first Compton interaction is 0.59 Mev.

Since we have seen that in attenuation of the gamma ray, high energy electrons are produced, it is of interest to examine the interaction of these particles with matter.

In its passage through matter an energetic electron will experience electrical interactions with external (orbital) electrons of the atoms of the absorbing matter. As a result of this electrical interaction, some of the energy of the energetic electron will be transferred to the external electrons. If the energetic electron possesses sufficient energy and it passes close enough to the external electron, the energy transfer will be sufficient to tear the external electron away from the atom. If this occurs there remains a positively charged atom or positive ion. The positive ion and separate electron are called an ion pair. This interaction may be written as follows:

$$e + e_{bound} \rightarrow 2e \qquad \text{(ionization)}$$

However, if the energy transfer is not sufficient to remove the external electron from the atom, excitation will occur. This means that the

external electron will still remain bound to the atom but will be in an excited or higher energy state. This interaction is written as follows:

$$e + e_{bound} \rightarrow e + e^{*}_{bound} \qquad \text{(excitation)}$$

The energetic electron may also have electrical interactions with the nucleus of the atom. This is known as Rutherford scattering. If the electron possesses sufficient energy (a few hundred kev) it may cause the displacement of the atom from its lattice position in a crystal lattice. This process may be written as:

$$e + N \rightarrow e + N_{displaced} \qquad \text{(dislocation)}$$

As a result of electrostatic interaction with the atomic nuclei and with electrons, high energy electrons do not travel in straight lines but scatter after interactions in different directions.

These particles may lose energy by the production of Bremsstrahlung or Cerenkov radiation; but as this is only important for energies greater than of interest here we shall not investigate this phenomenon.

At any rate, the end result of gamma interactions is to impart latent energy to the crystal (in the case of LiF) which is released by heating the crystal and possibly to cause defects in the crystal structure.

Excited Electron Storage [1] [3]

In order for the thermoluminescent phenomena to occur, the excited electrons must enter into a metastable state. Although the exact cause of the metastable states is not known, there are several suggested models to explain this phenomena.

After having caused the appearance of a few vacancies and interstitial ions, the γ radiation has transferred most of its energy to the electrons of the crystal. Among these electrons some have sufficient energy to occupy sites in the continuum (i.e., $E_e > E_i$). Through inelastic shocks with less energetic electrons, the initial energy is distributed among an increasing number of electrons. In addition, the radiation loses a great part of its energy in the production of phonons and photons. Although these phonons and photons may pass from the system, these are not the only possibilities. A few of the possible fates of the photons or phonons are listed as follows:

a. If the energy of the photon is slightly greater than the width of the forbidden band an electron hole-pair may be formed. Each of these carriers may then diffuse in the crystal until they recombine directly with a carrier of the opposite sign (unlikely) or they are trapped by a lattice defect. Depending on the type of defect and even upon the quantum state there will be:

    1. Recombination with a carrier of opposite sign;

    2. Ejection in the closest energy band;

    3. Transition to a state of smaller energy where the carrier is trapped until further stimulation.

b. The photon may produce an exciton. Although the final end of the exciton is still unknown the following are two reasonable possibilities:

1. Capture close to a dislocation where the survival of other excitons accumulate enough energy to dislodge an ion and create defects of the Schottky or Frenkel types;

2. Capture by halogen vacancy, with the production of an F center and a free hole.

The net effect of the energy degradation is that the average energy of the electron decreases progressively and eventually all the electrons are in the excited state such that $E_e < E_i$.

Figure 10 is a hypothetical energy diagram of an insulating crystal exhibiting thermoluminescence due to ionizing radiation. An electron in the valance band is excited to a higher state leaving a hole in the conduction band. The electron and hole then move about in the crystal, losing energy either by photon or phonon emission until they recombine or are trapped in a metastable state. These metastable states are presumed to be associated with the defects and resulting wave-function disturbances in the crystal. The particular type of metastable state into which an electron enters depends upon both the type of defect and the quantum state of the electron and defect.

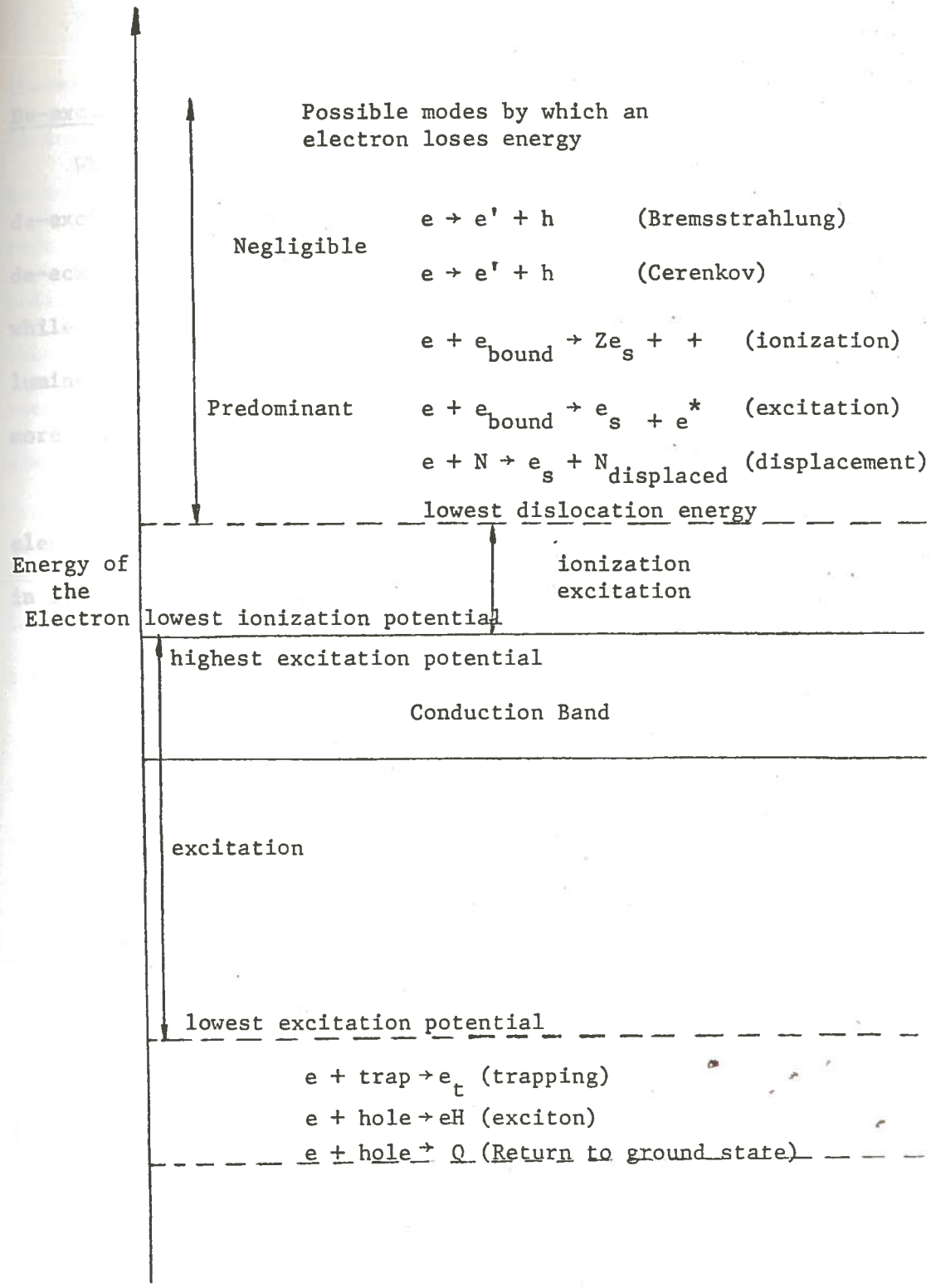

Figure 10. Energy Distribution Diagram

De-exciation of Trapped Electrons [1] [3] [6]

When an electron is released from its metastable state it may de-excite either radiatively or non-radiatively. An electron which de-ecxites radiatively contributes to the luminescence of the crystal, while a non-radiative de-excitation contributes nothing to the luminescence. We now wish to examine the models of de-excitation more closely.

First let us imagine that following some circumstance the electronic configuration diagram for the metastable state appears as in figure 11. Let us now suppose that the electron is in the excited

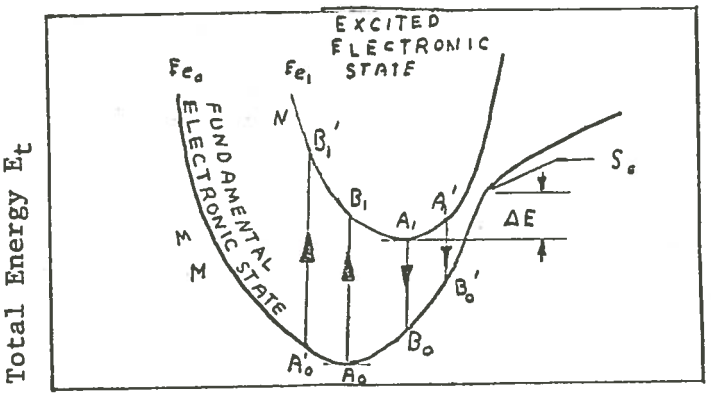

Figure 11: Configuration Diagram

electronic state centered around A_1. If the transition from A_1 to B_0 is not permitted, then the electron at energy state A_1 is said to be metastable*. If the thermal energy of the electron is increased, the

*An electron said to be in state A_1 is actually gravitating around state A_1 because of thermal vibrations. However, at low temperatures the difference due to these thermal vibrations is small and may be considered negligible.

thermal phonons may raise the energy of the electron close to that pictured by S_1 (figure 11). In this state any carrier may make the transition from state S_1 to state S_0. It will then successively pass through the states located along the arc S_0A_0, while emitting phonons until it returns to the ground state S_0 (after the crystal has cooled). Thus the system has passed from an excited electronic state to a non-excited state without the emission of photons. This is an example of a nonradiative transition.

Of particular interest are the radiative de-excitations. There are two prominent models of radiative de-excitation. They are thermo-luminescence due to an isolated luminescent center, and luminescence accompanied by photoconductivity.

In the first of these models we consider an electronic configuration diagram as in figure 12. We have seen how the thermal vibrations could

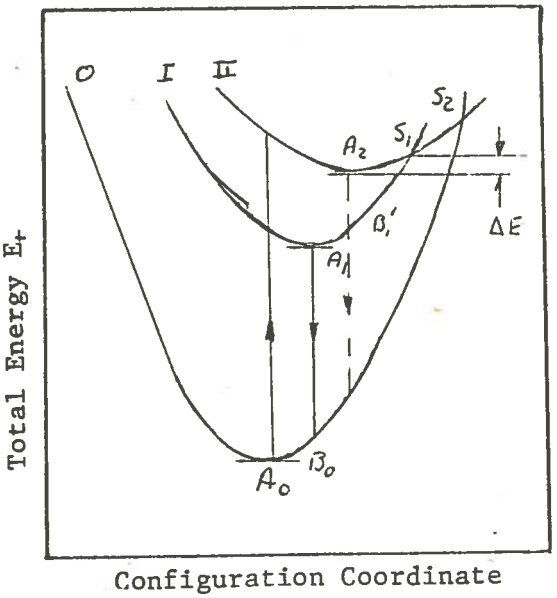

Figure 12. Configuration Diagram

cause nonradiative transitions, but there is also another possibility: the system may pass to another excited state. Figure 12 presents just such a possibility. The two upper curves are two different excited electronic states I and II. Let us first consider the case where a carrier is initially in state II centered around A_2. Let us further suppose that the optical transition from A_2 to B_0' and A_2 to B_1' are forbidden. Under these conditions if $KT << \Delta E$, the system will almost indefinitely remain in this state. But if the crystal temperature increases so that KT becomes comparable to ΔE, then the carrier may pass to state S_I, from which it immediately falls back to A_1. If the transition $A_1 \rightarrow B_0'$ is permitted, there will result a transition from A_1 to B_0 accompanied by the emission of a photon. In other words, under the thermal excitation (heat) an important part of the stored excitation energy will be released in the form of light. This is thermoluminescence.

We may picture the thermoluminescence accompanied by photoconductivity by the following schematic description.

There exists a certain number of activation centers, each of which has, in the absence of any excitation, an electron in a state close to the valence band (figure 13); the sequence of events follows:

1. By absorption of photon of energy, $E \geq Eg$ there is the creation of a pair of free carriers;
2. The hole is trapped by an activation center, with dissipation of a small energy E_i in the form of phonons.
3. An electron of the conduction band passing close to the center makes a radiative transition by recombining with the hole.

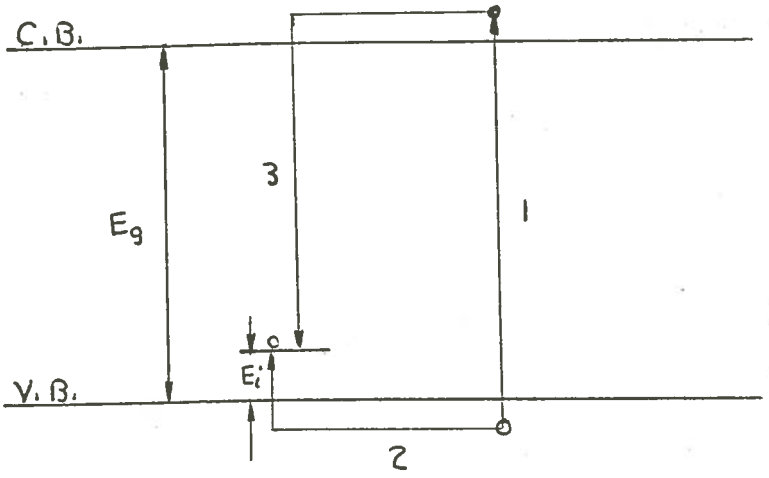

Figure 13. Model of Photoluminescence

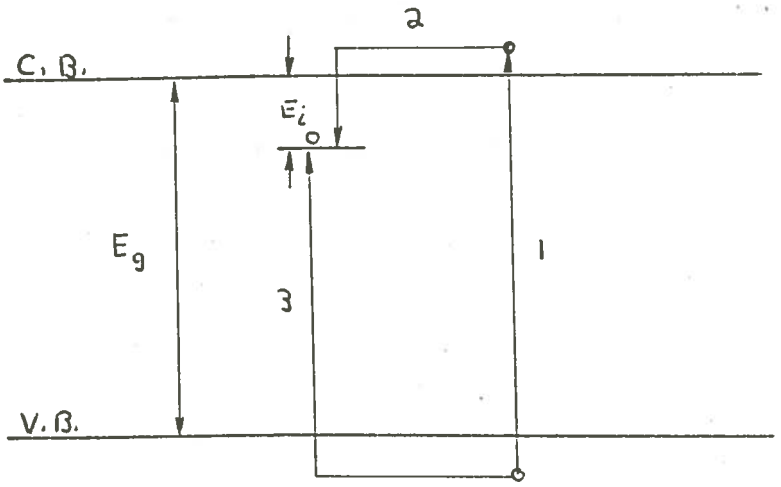

Figure 14. Model of Photoluminescence

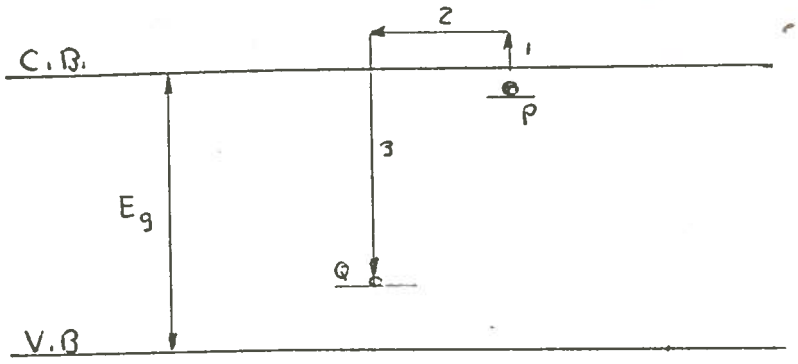

Figure 15. Model of Thermoluminescence

Also the electron may be trapped at a level close to the conduction band and later recombine with the hole with the emission of a luminescent phonon. See figure 14.

From the point of view of thermoluminescence (with photoconductivity) it is easy to imagine acceptable schematic mechanisms. For example, following excitation there would be electrons and holes staying in centers such as P + Q (figure 15) in one or several metastable levels. Thus the centers P are electron traps, the centers Q hole traps.

Following an increase in temperature and by a mechanism quite similar to that described of the isolated luminescent centers, (transition A_1 to S_1, figure 12) the electron of trap P would be brought into the conduction band. Being almost free in the conduction band, it would move at random, under the influence of shocks from phonons, until there was either a retrapping by a center of the same nature P, or a radiative transition in an activation center Q containing a hole.

Thus we have seen, qualitatively, the dependence of luminescence upon temperature. Randall and Wilkins [6] developed a similar first order kinetics model for thermoluminescence. According to the model, each peak of the glow curve is related to a trap with a trap depth E and a frequency factor S. For a constant temperature, the number of remaining trapped electrons (N) for a given peak is a function of time (t). The mathematical model of this development is:

$$N = N_o \exp\left[(-st)\exp(-E/KT)\right],$$

where N_o = initial number of trapped electrons

K = Boltzman's constant

T = absolute temperature

t = time

s = frequency factor.

Criteria of Model [1]

A successful model for the thermoluminescence phenomenon should be able to predict the thermoluminescence response of the dosimeter, at least in a qualitative fashion. In addition, it should not conflict with any known phenomenon so as to make the proposed model incompatible with experimental evidence.

In summary, the model should explain the following:

1. Lithium fluoride has a linear dose response to about 10^3 R, then a supralinear region to approximately 2.5×10^4 R. Above this dose the response of the dosimeter decreases, and actually shows reversal. (See figure 16).

2. When a 400°C anneal is used following radiation exposure, a loss of response (i.e., radiation-induced damage) is noted after about 10^3 R. This damage is noticiably increased if there are several annealings is the exposure history of of the dosimeter. (See figure 17).

3. If an annealing temperature of 280°C or less is used, the response of the dosimeter is enhanced. (See figure 18).

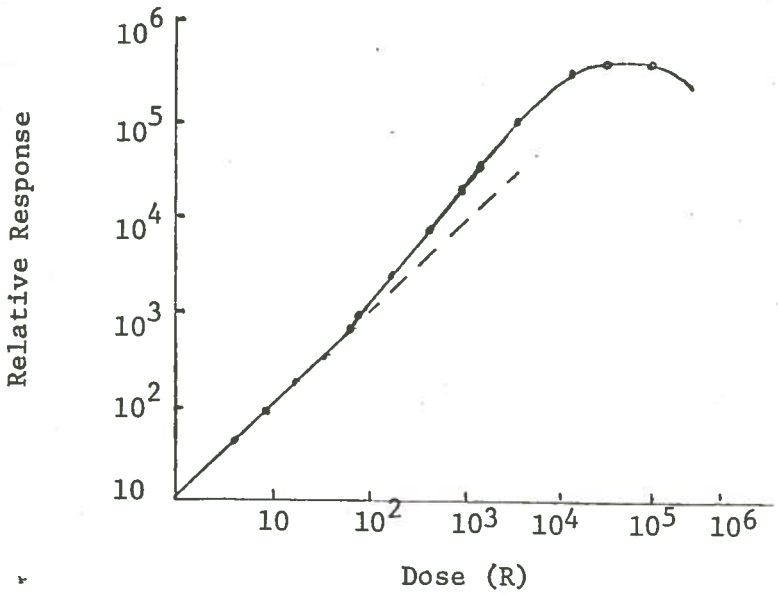

Figure 16. Response of LiF

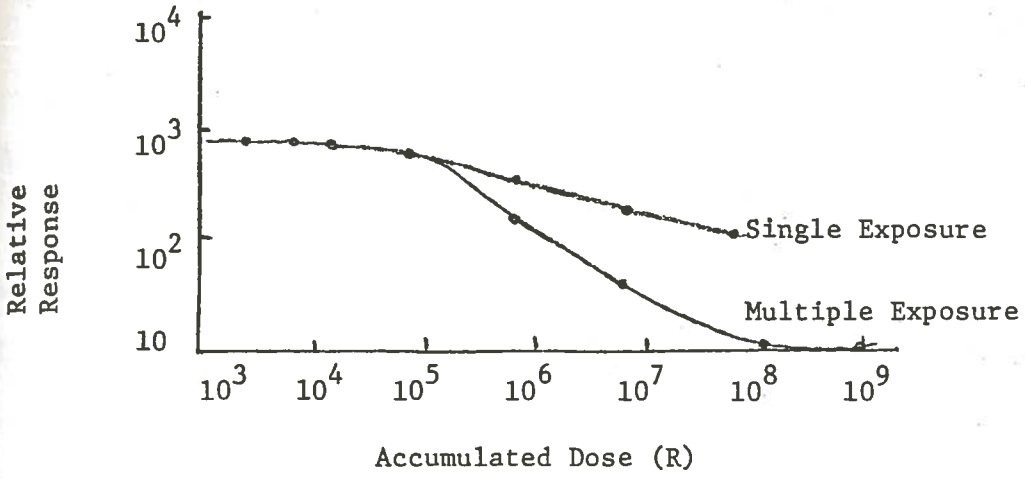

Figure 17. Damage of LiF

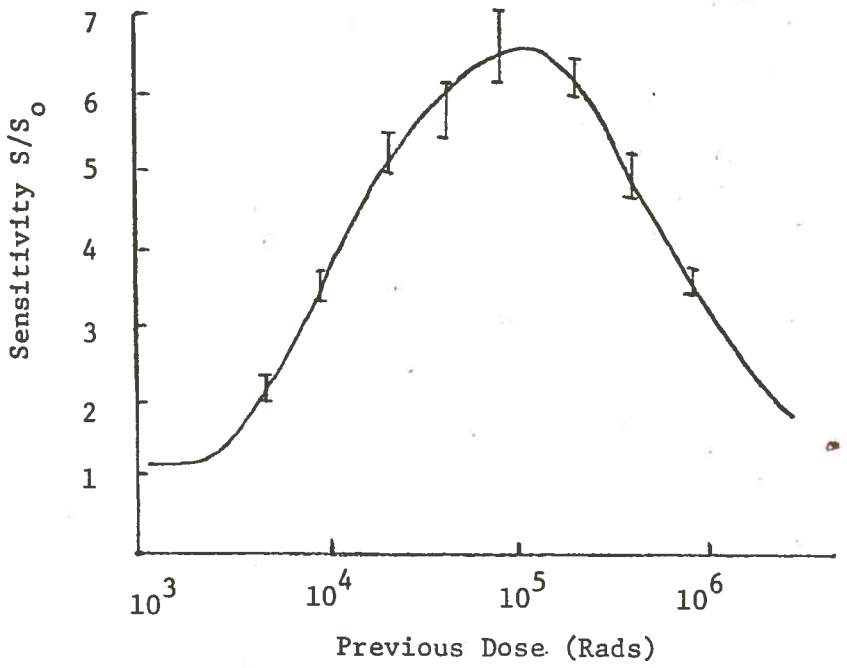

Figure 18. Sensitivity of LiF Vs. Exposure Following a 280°C Anneal

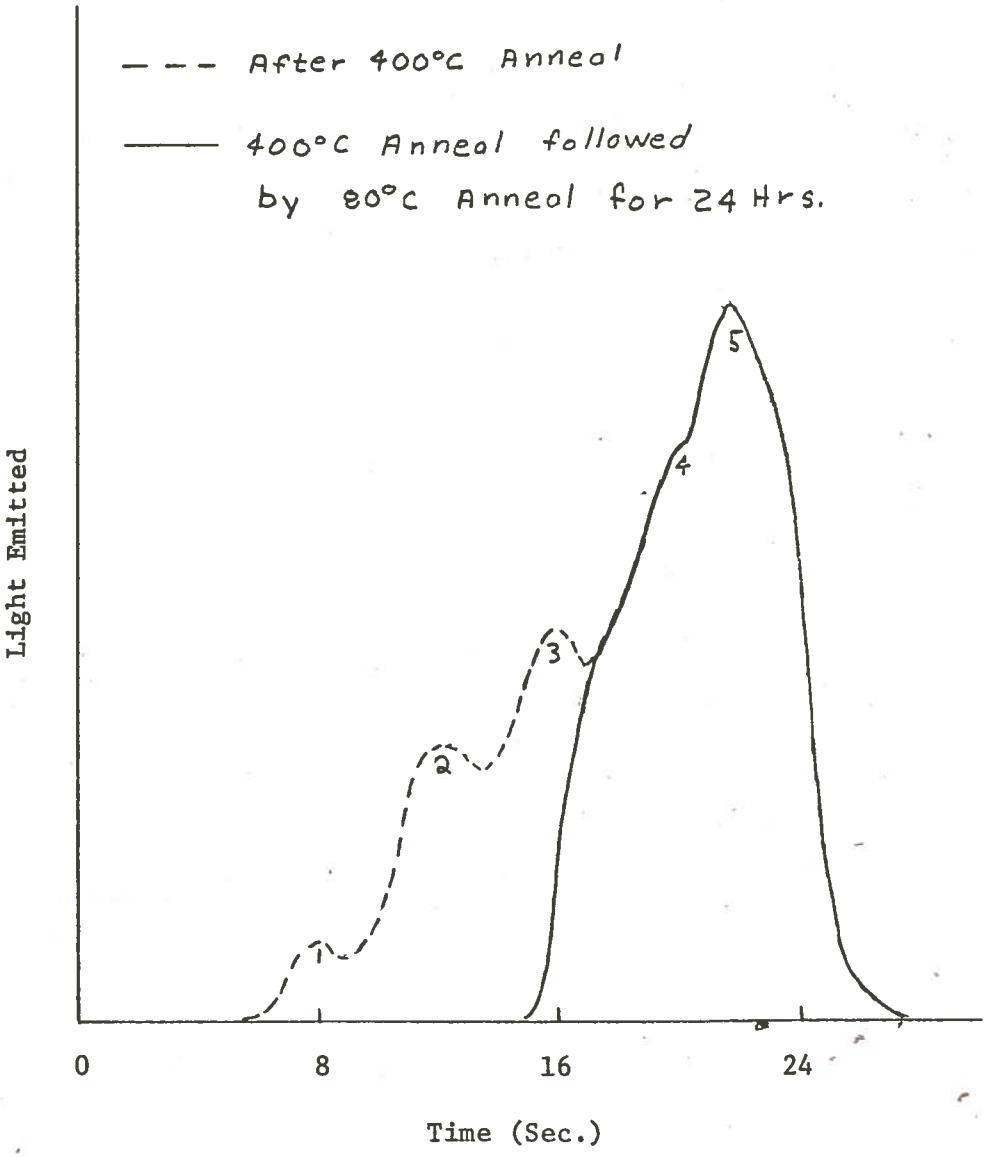

Figure 19. Glow Curves of LiF

Experimental Evidence [1]

The model which will be developed will be based on the experimental observation and work mentioned in this section. The particular dosimeter of interest in this development will be LiF TLD 100 which contains 7.5% ^{6}Li and 92.5% ^{7}Li. A dosimeter which has had no exposure to radiation, but has been annealed at 400°C for one hour followed by rapid cooling and subsequent anneal at 80°C will be denoted as a virgin dosimeter. The above mentioned heat treatment is that developed by J. R. Cameron at the University of Wisconsin, and has come to be considered the standard treatment for LiF dosimeters.

In his book, Thermoluminescent Dosimetry, J. R. Cameron enumerated typical characteristics of LiF TLD 100 thermoluminescent dosimeters. Of interest in this development are the following:

1. A typical glow curve of TLD 100 has five peaks as shown in figure 19. After irradiation, peaks 1 through 5 decay at varying rates at room temperature. The half life of the peaks are: peak 1, 5 minutes; peak 2, 10 hours; peak 3, 0.5 year; peak 4, 7 years; and peak 5, 80 years. The standard heat treatment almost entirely removes peaks 1 and 2 and lessens the effect of peak 3. The same effect can be achieved by post-irradiation annealing for 1 hour at 100°C. Therefore, for the purpose of this study we shall consider the glow curve consisting of only peaks 4 and 5.

2. The emission spectra for LiF has a broad spectrum with a single peak at $\simeq$ 4000 A.

3. The exposure response curve (figure 16) is linear up to approximately 10^{3} R, beyond which it becomes superlinear until it plateus at approximately 5×10^{5} R and then decreases with increasing exposure.

4. No dose rate effect has been noted.

5. The trap depth of peak 4 is 1.19 ± 0.5 ev, and of peak 5 is 1.25 ± 0.6 ev. The frequency factor for peak 4 is 1.0 - 15 (10^{-11} x sec^{1}); and peak 5, 0.5 - 14 (10^{-11} x sec^{1}).

6. Cameron listed three possible explanations for the super-linearity of LiF. They are:

   a. Creation of additional trapping sites;

   b. Creation of new recombination centers;

   c. An increase in Tl efficiency.

7. Using the ratio of S/S_o as an indication of sensitivity the response of TLD 100 after exposure to 10^5 R of Cs^{137} gamma radiation and annealed at 280°C for 0.5 hour, the response is increased by a factor of 6 for a 100 R exposure. (See figure 18). If the dosimeter is annealed at 400°C for 1 hour, the increase in sensitivity is removed. The sensitivity of LiF after exposure to 10^4 R of Cs^{137} gamma radiation for various annealing times is shown in figure 20. The inactivation energy E is 2.1 ± 0.35 ev, which is on the order the disassociation energy of the F_1 center. However, no definite conclusion can be made about the nature of the site.

8. The response of LiF decreases after exposure of greater than 2 x 10^4 R, followed by 400°C anneal. The loss of sensitivity as a function of exposure is shown in figure 17. For multiple exposures to Cs^{137} gamma radiation there is greater damage for the same total exposure. (See figure 17).

9. An interesting interpretation of the double exponential curve shown in figure 21 is that the amount of radiation-induced loss of sensitivity in LiF differs for filled traps and for unfilled traps. The rapidly decreasing exponential can be attributed to damage to unfilled traps, while the slower component is attributed to damage to the filled traps. The developed empirical equation for S/S_o as a function of dose is:

$$S/S_o = 0.60 \exp(-.250553 \times 10^{-4} R) + 0.40 \cdot \exp(-.26 \times 10^{-6} R)$$

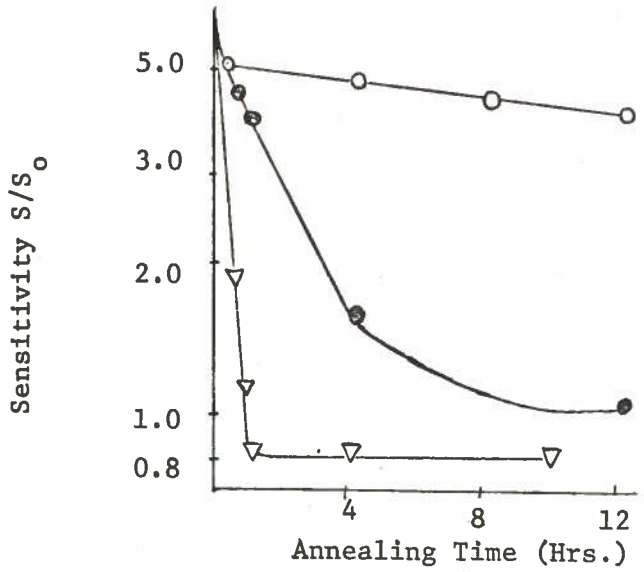

Figure 20. Sensitivity as a Function of Time and Annealing Temperature

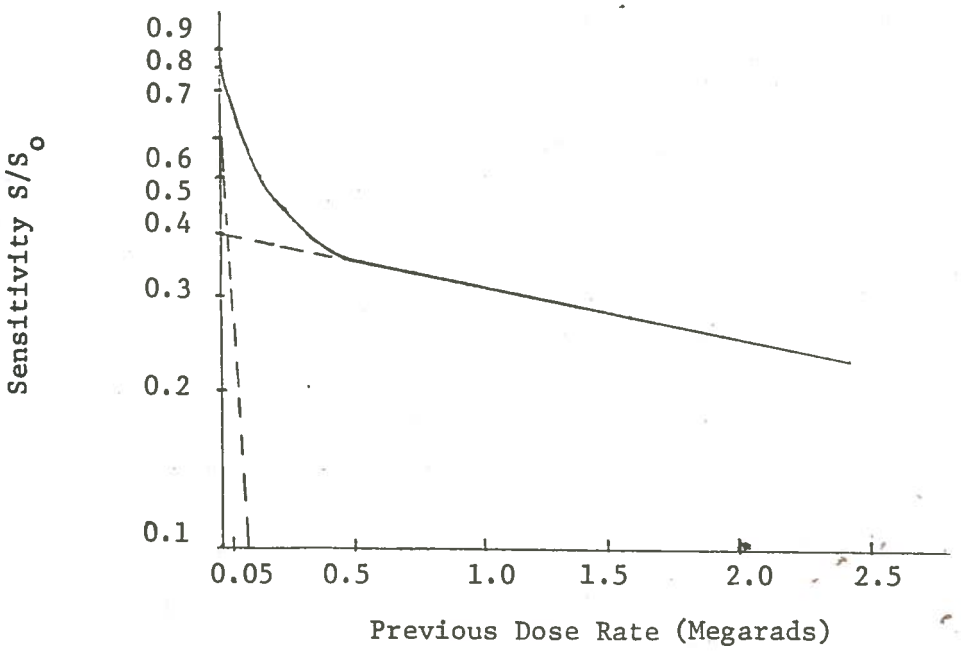

Figure 21. Damage as a Function of Exposure

Development of Model [1]

After the standard heat treatment there are two peaks in the glow curve. To each peak we shall assign a trap type, type A and trap B respectively. The following notation shall be used:

A_o = # of original traps of type A

B_o = # of original traps of type B

A^* = # of excited traps of type A

B^* = # of excited traps of type B.

An excited trap is one which has trapped a carrier and is a center for thermoluminescence. All of the excited traps may not dump the carriers under the readout. However if we assume: (1) reproducible readout heat cycle; (2) linear response of the photomultiplier tube; and (3) constant geometry, we see that the response of the tube should be directly proportional to the number of excited traps.

In the development of the model it is assumed that under the influence of radiation traps A and B may be transformed into trap types C and D, respectively. C and D may be either nonradiative traps or traps which dump radiatively at a temperature much greater than the readout temperature. Further, traps C and D do not anneal out or transform back into A and B at a 400°C anneal temperature (1 hour anneal).

In addition to these traps there is another type of trap denoted as traps E, and F. These traps act to prevent the radiative release of traps A and B. They may be pictured as acting in the following

manner: Upon release of a carrier by a radiative trap the carrier is subsequently trapped by either trap E or trap F. The carrier is trapped before it has completed a radiative transition and therefore does not contribute to the response. When the traps (E or F) has trapped one carrier they can no longer trap another carrier. This trap (E or F) returns to its ground state during a 400°C anneal, but not as a result of a 280°C anneal.

In summary we shall propose that the response of the crystal may be expressed as:

$$S = \varepsilon(\alpha A^* + \beta B^* - E^* - F^*)$$

where ε = proportionality constant for photomultiplier tube

α = fraction of A^* released in readout

β = fraction of B^* released in readout.

It has been assumed that ε is the same for both A^* and B^*. Justification for this assumption is the fact that the wavelength of emitted light is the same for both traps.

We now wish to develop an expression for A^* and B^*. Consider the following:

$$\frac{dA}{dR} = -K_1 A - C_1 A$$

where K_1 = rate of conversion to A^*

C_1 = rate of conversion to C

R = radiation dose

Solution: $A = A_o e^{-(K_1 + C_1)R}$

Similarly, $\frac{dB}{dR} = -K_2B - C_2B$

where: K_2 = rate of conversion to B^*

C_1 = rate of conversion to D

Solution: $B = B_o\, e^{-(K_2 + C_2)\, R}$

Now, $\frac{dA^*}{dR} = K_1A - C_3A^*$

where: C_3 = rate of conversion to C^*

Solution: $A^* = \frac{K_1A_o}{K_1 + C_1 - C_3} \left(e^{-C_3R} - e^{-(K_1 + C_1)R}\right)$

Similarly, $B^* = \frac{K_2B_o}{K_2 + C_2 - C_4} \left(e^{-C_4R} - e^{-(K_2 + C_2)R}\right)$

where: C_4 = rate of conversion to D^*

Consider now E^* and F^*, allowing the possibility of conversion by radiation:

$\frac{dE}{dR} = C_5R$

where: C_5 = rate of conversion of E

Solution: $E = e^{-C_5R}$

Now, $\frac{dE^*}{d(\alpha A^*)} = K_3E$

where: K_3 = rate of filling during readout

Solution: $E^* = E_o e^{-C_5R} \left(1 - e^{-K_3(\alpha A^*)}\right)$

Similarly, $F^* = F_o e^{-C_6R} \left(1 - e^{(-K_4\beta B^*)}\right)$

where: C_6 = rate of conversion of F

K_4 = rate of filling during readout

Thus, $$S = \varepsilon(\alpha A^* + \beta B^* - E^* - F^*)$$

where: $$A^* = \frac{K_1 A_o}{K_1 + C_1 - C_3} \left(e^{-C_3 R} - e^{-(K_1 + C_1)R}\right)$$

$$B^* = \frac{K_2 B_o}{K_2 + C_2 - C_4} \left(e^{-C_4 R} - e^{-(K_2 + C_2)R}\right)$$

$$E^* = E_o e^{-C_5 R} \left(1 - e^{-K_3 \alpha A^*}\right)$$

$$F^* = F_o e^{-C_6 R} \left(1 - e^{-K_4 \beta B^*}\right)$$

Test of Model

In order to test the model, data from the literature which is considered the best available will be employed. Three tests of the model can be made:

1. The response over the full range of exposure which should coincide with both the linear and supralinear region.
2. The effect of damage in single and multiple exposures.
3. The increase in sensitivity.

The data employed for testing the model are taken from the curves published by Cameron and others.

Data employed for these tests are based upon integration of peaks number 4 and 5 (see figure 19). Integration over these two peaks precludes the possibility of separating the effects of the A and B type traps, and of the E and F type traps. Therefore the model developed in the preceding section will be simplified by the assumption of a single type of radiative trap (i.e., $A = A + B$, $A^* = A^* + B^*$), and a single scavenging trap (i.e., $E = E + F$, $E^* = E^* + F^*$). Based upon these simplifications, the equation describing the response is:

$$S = \frac{K_1 A_o}{C_1 + K_1 - C_2} \left(e^{-C_2 R} - e^{-(C_1 + K_1)R}\right)$$

$$- E_o \left(1 - e^{-C_3 A^*}\right) e^{-C_4 R}$$

where K_1 = rate of filling of radiative traps

C_1 = rate of conversion of empty radiative traps

C_2 = rate of conversion of filled radiative traps

C_3 = rate of filling scavenger traps

C_4 = rate of conversion of scavenger traps

A_o is the original number of radiative traps reduced by a factor = $\varepsilon\alpha$

Test I: Response vs. Dosage.

Empirical fitting of the response equation by trial and error determination of the various constants has led to the following values:

$A_o = 1.43 \times 10^6$

$E_o = 9.30 \times 10^6$

$K_1 = 1.0 \times 10^{-5}$

$C_1 = 1.5 \times 10^{-5}$

$C_2 = 2.6 \times 10^{-7}$

$C_3 = 1.0 \times 10^{-7}$

$C_4 = 9.0 \times 10^{-6}$.

The values for K_1, C_1, and C_2 are those obtained from Cameron. Thus the response equation is:

$$S = 572{,}500 \left(e^{-2.6 \times 10^{-7} R} - e^{-2.5 \times 10^{-5} R}\right) - 9{,}300{,}000\, e^{-9.0 \times 10^{-6} R} \left(1 - e^{-1.0 \times 10^{-7} A^*}\right)$$

where: $$A^* = 572{,}500 \left(d^{-2.6 \times 10^{-7} R} - e^{-2.5 \times 10^{-5} R}\right)$$

In table I the values calculated by the response equation are compared with the response curve reported by Cameron. These values and data are plotted in figure 22. The maximum difference between the computed values and the experimental data is 11.9% at a dose of 300,000 R; all other points differ by less than 6%. As shown in figure 22 the model provides a reasonable fit of the experimental data, that is, the response is linear to approximately 1,000 R, passes into a supralinear region, and ultimately shows a reversal. The variation of A^* and E^* with dose are also shown in figure 22.

Test 2: Radiation Damage.

A second test of the model would be a comparison between the predicted damage due to radiation and the experimentally observed damage. It was assumed that all of the filled scavenger traps, E^*, were emptied following a two hour anneal at 420°C, but that none of the radiative traps which had been transformed to nonradiative traps were returned to their original state. Thus the theoretical damage would be due to the conversion of unfilled traps and the conversion of filled traps. For a single exposure the damage is expressed as:

$$S/S_o = 0.60 \exp(-2.5 \times 10^{-5} R) + 0.4 \exp(-2.6 \times 10^{-7} R)$$

For multiple exposure it is necessary to calculate the damage due to each exposure and then to multiply to obtain the cumulative damage:

$$S/S_o = 0.60 \exp(-2.5 \times 10^{-5} R_1) + 0.40 \exp(-2.6 \times 10^{-7} R_1)$$

TABLE I

RESPONSE VS. DOSAGE [a]

Dose (R)	A*	E*	Predicted Response	Response From Graph	% Error
10	143	133	10	10	0
100	1,432	1,331	101	100	0.1% high
1,000	14,165	13,046	1,119	1,100	1.7% high
3,000	41,454	37,447	4,007	4,200	4.6% low
6,000	79,014	69,345	9,669	10,050	3.8% low
10,000	125,395	105,915	19,480	20,000	2.6% low
20,000	222,674	171,062	51,612	51,000	1.2% high
40,000	356,430	227,192	129,238	122,000	5.9% high
60,000	436,319	231,381	204,938	200,000	2.5% high
80,000	483,576	213,696	269,880	260,000	3.8% high
100,000	511,071	188,386	322,685	310,000	4.1% high
200,000	539,674	80,764	458,910	410,000	11.9% high
300,000	529,320	32,217	497,013	490,000	1.4% high
500,000	502,706	5,065	497,641	500,000	0.5% low

a. Calculated values are reported complete without regard for significant figures. Three significant figures are justified.

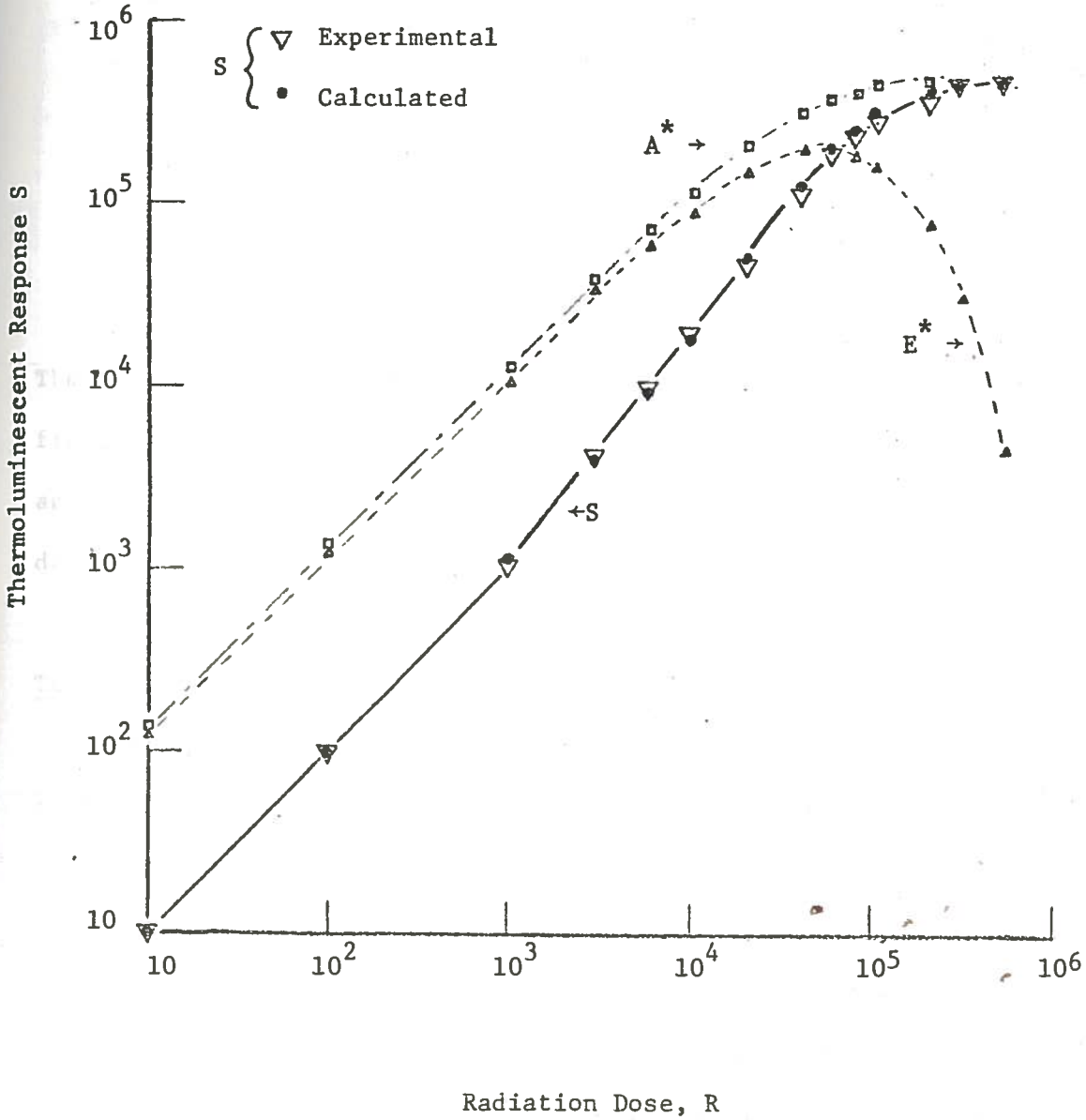

Figure 22. Comparison of Predicted and Experimental Response of LiF and abundance of Radiative and Scavenging Traps

therefore $0.60 \exp (2.5 \times 10^{-5} R_2) + 0.40 \exp (-2.6 \times 10^{-7} R_2)$

.

.

.

where: R_1 = dose obtained in first exposure

R_2 = dose obtained in second exposure

.

.

.

The results of these calculations are listed in table II and plotted in figure 23. The theoretically predicted damage for a single exposure agrees well with the experimental results. However, the predicted damage for multiple exposures is overestimated by the model.

Test 3: Increased Sensitivity.

As a final test of the model, a comparison can be made between the predicted and experimental results of the sensitivity of an exposed crystal following a one hour anneal at 280°C. It is assumed that this temperature is not sufficient to cause E^* to return to its ground state. The results are tabulated in table III and plotted in figure 24. Although the calculated sensitivity (curve A) does not agree well with the experimental data (curve B), the shapes of the two curves are in reasonable agreement. This can be seen from the normalized model curve (C) which was obtained by multiplying the sensitivity by a factor of 1.293 and the dosage by a factor of .325.

TABLE II

DAMAGE VS. DOSE

Total Dose	S/S_o, Single Exposure		S/S_o, Multiple Exposure	
	Predicted	Experimental	Predicted	Experimental
3.0×10^4	.68	.68	.68	.68
6.0×10^4	.53	.53	.47	.53
9.0×10^4	.45	.45	.32	.45
1.2×10^5	.42	.42	.22	.38
1.5×10^5	.40	.40	.15	.36
1.8×10^5	.39	.39	.10	.33
2.1×10^5	.39	.38	.07	.3
2.4×10^5	.38	.37	.05	.28

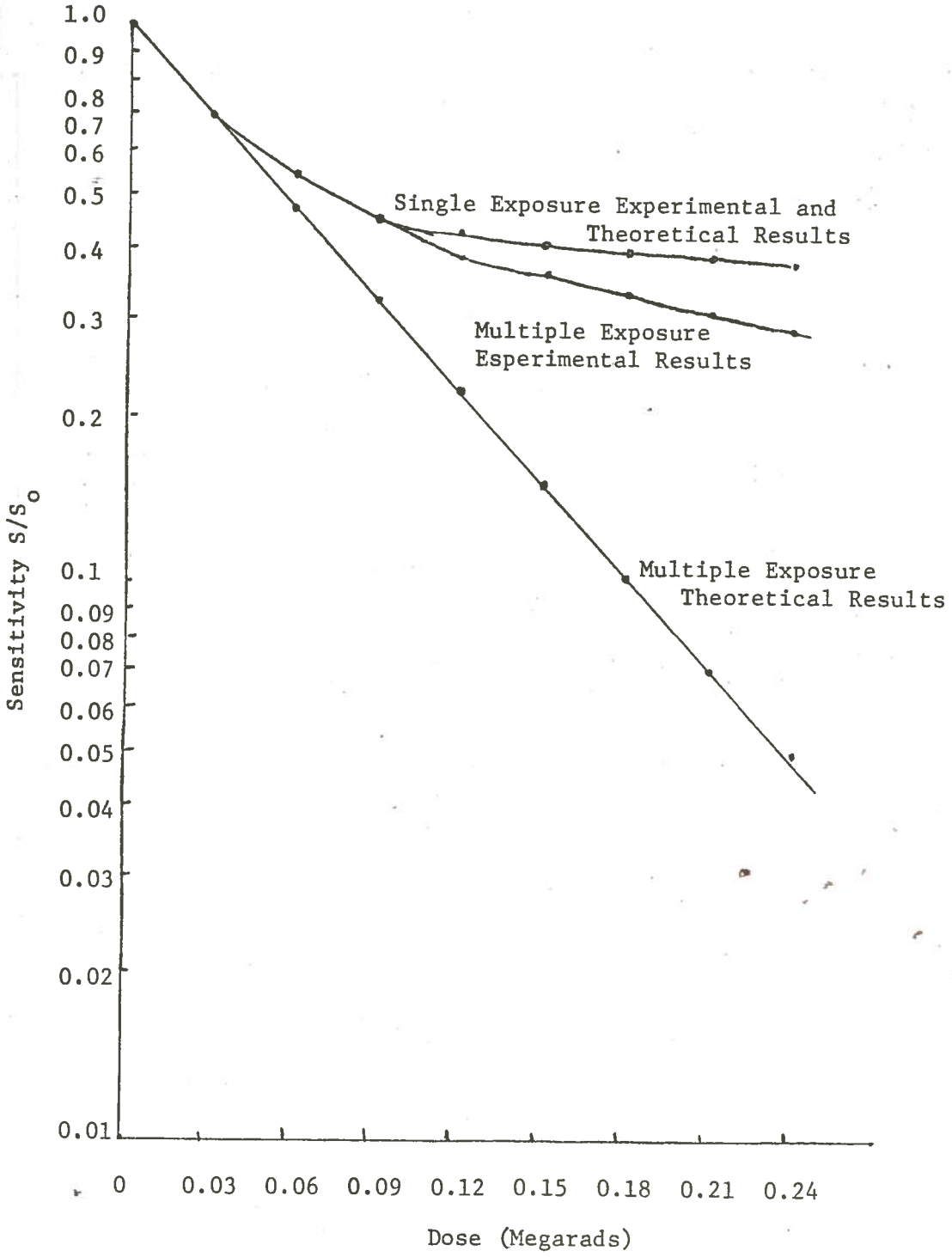

Figure 23. Comparison of Predicted and Experimental Damage of LiF

TABLE III

INCREASE IN SENSITIVITY
AS A FUNCTION OF DOSE
FOLLOWING A 280°C ANNEAL [a]

Previous Exposure (R)	Predicted				S/S_o	
	A^*	E^*	Response	S/S_o	Experimental	Normalized
1,000	1,410	1,296	114	1.14	1.2	N.A.
5,000	1,330	1,173	156	1.56	1.6	3.0
10,000	1,240	1,040	200	2.0	3.4	3.65
40,000	822	514	308	3.08	5.2	5.5
100,000	628	225	403	4.03	6.4	6.45
200,000	550	80	470	4.7	6.2	6.3
300,000	530	31	499	4.99	5.8	5.8
400,000	506	5	501	5.01	5.35	5.4
500,000	502	5	497	4.97	4.9	5.0
1,000,000	441	0	441	4.41	3.3	3.8
10,000,000	42.5	0	42.5	0.425	N.A.	N.A.

a. Calculated values are reported complete without regard for significant figures. Three significant figures are justified.

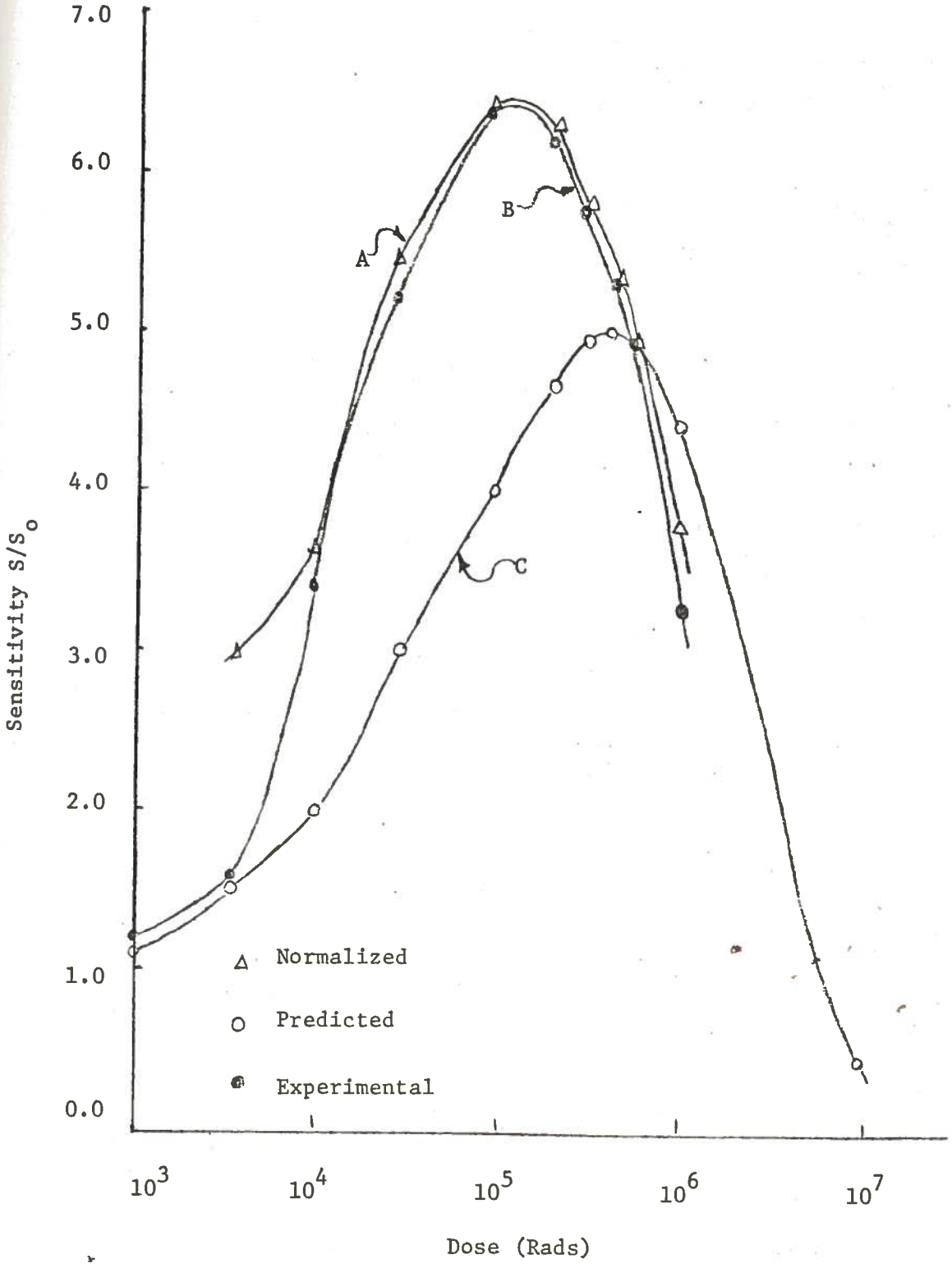

Figure 24. Comparison of Predicted and Experimental Sensitivity of LiF

DISCUSSION

Cameron has summarized the requirements for an adequate model to describe the behaviour of LiF as a thermoluminescent material and has discussed critically some of the previously proposed mathematical models [1]. Among the possibilities discussed are:

1. The creation of additional trapping sites;
2. The creation of new recombination centers;
3. An increase of thermoluminescent efficiency, which would coincide with a decrease in nonradiative transistions.

A search of the literature has revealed only those models reported by Cameron in his book, Thermoluminescent Dosimetry. The first model which Cameron developed was based upon the assumption that the supra-linear response of LiF was due to the creation of additional trapping sites and upon the hypothesis of the existance of a maximum trap density. The resulting solution gives a very good fit to the response curve of LiF. For exposures less than 4×10^5 R, the greatest disagreement was only 3%. Despite the remarkable agreement of this model, Cameron felt that there was definite weaknesses in the model. The major weaknesses were the fact that the glow curve is essentially unchanged up to 10^5 R (during this time the number of traps increase by a factor of 6) which implies that new traps are being created with the same relative proportions as the initial traps. Furthermore, the stability of the electrons in the created traps are the same as for those in the initial traps. Cameron considers that these are highly unlikely coincidences.

To overcome these difficulties, Cameron developed a model based upon the creation of additional recombination centers rather than traps. The main objection to this model is the fact that the emission spectra of the sensitized and unsensitized phosphors indicate that the created recombination centers are essentially identical to the initial recombination centers. Cameron also considers this an unlikely coincidence.

In addition to Cameron's criticism it is noted that neither of the models would account for the reversal of the response curve, or for the damage to the phosphor after exposure.

The model proposed in this thesis corresponds with Cameron's third suggestion which he has not developed mathematically. For purposes of this discussion, and to distinguish it from other models, it will be referred to as the scavenger-trap model. The basic premises are:

1. There exists in LiF scavenging traps which intercept the electrons from radiative centers during the read-out cycle and prevent photon emission;
2. Electrons remain in the scavenger traps until the LiF is heated to temperatures in excess of 300°C;
3. At annealing temperatures in the region of 400°C the electrons in the scavenger traps are returned to the ground state;
4. The number of scavenger traps is limited.

These premises provide an interpretation which accounts for the supra-linearity and sensitization of the LiF. However they are inadequate to acount for radiation damage. In order to build a description of radiation damage into the model it is further assumed that the radiative traps responsible for the thermoluminescence can be converted to non-

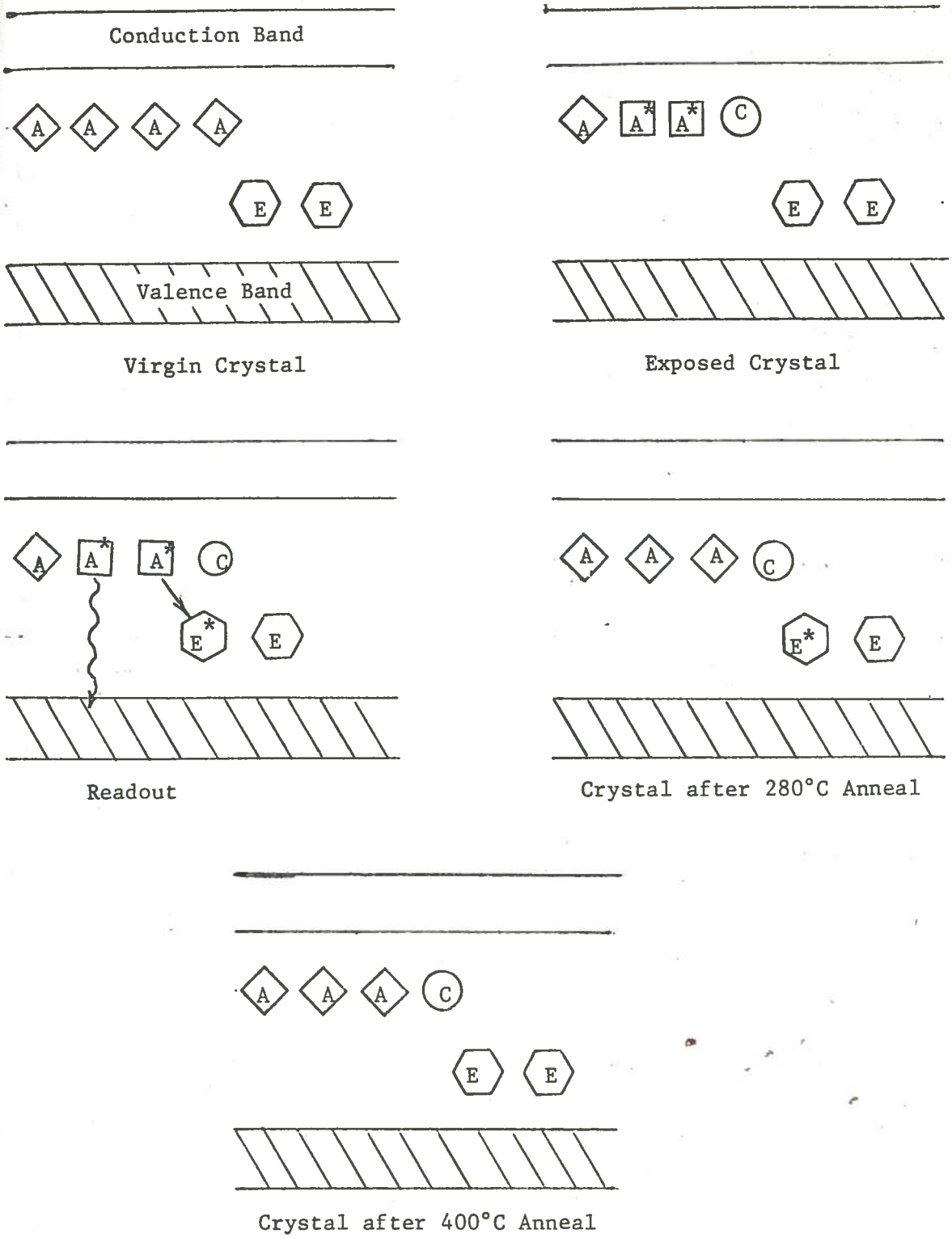

Figure 25. Pictorial Representation of Scavenger-Trap Model

radiative traps by exposure to radiation. The conversion is assumed to be more efficient for the empty radiative traps than for those which have captured electrons. Annealing at 400°C does not lead to restoration of the original trap, but restoration can be achieved by annealing at 600°C.

The qualitatitive aspects of this model are shown schematically in figure 25, assuming a single type of radiative trap, a single type of scavenging trap, and a single type of conversion trap.

In the mathematical development of the model, it is assumed that the processes involved in electron transitions and trap conversions follow psuedo first-order kinetics to simplify solution of the differential equations involved. It is recognized that the assumption of first order kinetics introduces errors, since, undoubtedly, some of the processes are probably second order at high doses. However, it is felt that the mathematical simplification is less severe than the assumption of single trap types. The shape of the glow curve for LiF strongly suggests a multiplicity of trap types involved in the radiative process, and there is no a priori justification for the existance of a single type of scavenging trap or a single type of conversion trap. It is believed that development of the model by involving a multiplicity of each trap type represents a refinement that cannot be adequately tested with available data.

At the present time, detailed theoretical knowledge of the radiation effects on LiF and the exact physical phenomena involved in thermoluminescence are not known. Consequently, a "first principles"

calculation of the constants involved in the mathematical description of the scavenger trap model cannot be made. The constants must therefore be determined empirically by trial and error. However, it is felt that empirical fitting of the derived equation to experimental data does not invalidate the test of the model. Since the variation of thermoluminescence response as measured experimentally by Cameron is fitted within an average error of approximately 3% over the range from 0 to 5×10^5 R, the model, even with its gross simplifications, cannot be completely wrong. The fact that the model reasonably predicts the shape of the dose sensitization curve provides further confidence in the basic premises. The major failure of the model is in describing the radiation damage curves. By modifying the model to account for the two peaks in the glow curve (i.e., by introducing both A^* and B^*) a reasonably accurate description can be calculated for both single-exposure and multiple-exposure damage. The development is as follows:

$$A + B = 1$$

$$A = 0.70 \qquad B = 0.30$$

let $\dfrac{K_1}{C_1 + K_1} = 0.1$ for A $\qquad \dfrac{K_2}{C_2 + K_2} = 1$ for B

let the conversion rate from A^* and B or B^* to a nonradiative trap be $= 2.6 \times 10^{-7}$.

let the conversion rate from A to a nonradiative trap be 2.5×10^{-5}.

The resulting expression for sensitivity for a single exposure is:

$$S/S_o = 0.3 \exp(-2.6 \times 10^{-7} R) + 0.7 [0.1 \exp(-2.6 \times 10^{-7} R) + 0.9 \exp(2.5 \times 10^{-5} R)]$$

The expression for multiple exposures is:

$$0.3 \exp(-2.6 \times 10^{-7} R) + 0.7 [0.1 \exp(-2.6 \times 10^{-7} R_1) + 0.9 \exp(2.5 \times 10^{-5} R_1)] \cdot [0.1 \exp(-2.6 \times 10^{-7} R_2) + 0.9 \exp(2.5 \times 10^{-5} R_2)] \ldots$$

where: $R = R_1 + R_2 + \ldots$

R_1 = dose due to first exposure

R_2 = dose due to second exposure

.

.

.

The results for these calculations are tabulated in table IV.

The model is not intended to predict in any absolute sense the number of photons emitted by the crystal--the constants which have been obtained by fitting to published curves pertain to these curves only since the thermoluminescence response is reported in arbitrary units. Furthermore, it is common experience that the response of LiF varies from batch to batch. In order to obtain absolute numbers for the abundances of the A and E traps it would be necessary to

TABLE IV

RADIATION DAMAGE VS. DOSE
FOR EXPERIMENTAL DATA AND TWO-TRAP MODEL

Dose	S/S_o Single Exposure		S/S_o Multiple Exposure	
	Predicted	Measured	Predicted	Measured
3.0×10^4	.66	.68	.66	.68
6.0×10^4	.51	.53	.51	.53
9.0×10^4	.43	.45	.42	.45
1.2×10^4	.39	.42	.36	.38
1.5×10^4	.37	.40	.33	.36
1.8×10^4	.36	.39	.33	.33
2.1×10^4	.35	.38	.30	.30
2.4×10^4	.35	.38	.29	.28

determine the absolute relationship between incident photon intensity and instrument readout. Furthermore it would be necessary to resolve the individual glow peaks before it would become possible to obtain numbers representing the photon yields from the participating radiative traps, and hence to calculate the abundances of the scavenger traps and the transition traps. Current techniques and current status of the instrumentation does not hold promise for complete experimental resolution of the individual glow peaks. Resolution of glow peaks would therefore have to be accomplished by empirical curve-fitting techniques, assuming some characteristic shape for the glow peak. It appears unlikely therefore, that information concerning the absolute number of traps of any kind can be obtained until more sophisticated techniques have been developed.

In the development of the model the temptation to identify known defect centers and trap types with the radiative, scavenging, and conversion traps has been avoided. Current knowledge of the details of the thermoluminescence process is too incomplete to make attempts to identify the traps meaningful. A critical test of the scavenger trap model developed here would be a specific search for the scavenger traps. If some experimental means of determining these traps can be discovered and the rate of filling of these traps measured and found to coincide with that predicted by this model, it would provide supporting evidence. Consideration of the techniques by which this might be accomplished is beyond the scope of this thesis.

SUMMARY AND CONCLUSIONS

This study was undertaken for the purpose of developing a better understanding of the response of thermoluminescent dosimeters. In particular, it was directed toward formulating a mathematical model to explain the response of LiF TLD 100 dosimeters to gamma radiation.

A mathematical model is based upon the following premises:

1. There exist two types of radiative traps;
2. There exist two types of scavenger traps;
3. The radiative traps may, under the influence of radiation be converted to nonradiative traps;
4. Depending upon temperature, the transformed radiative traps may or may not return to ground state;
5. There is a limited number of traps of both types.

The developed model for the response is:

$$S = A^* + B^* - E^* - F^*$$

where: A^* is a filled radiative trap and is computed by

$$A^* = \frac{K_1 A_o}{K_1 + C_1 + C_3} \left(e^{-C_3 R} - e^{-(C_1 + K_1)R}\right)$$

where: K_1 = rate of filling of radiative trap A

C_1 = conversion factor for empty traps

C_3 = conversion factor for filled traps

A_o = original number of traps of type A

for B^*, a second type of radiative trap:

$$B^* = \frac{K_2 B_o}{K_2 + C_2 - C_4} \left(e^{-C_4 R} - e^{-(C_2 + K_2)R}\right)$$

where: K_2 = rate of filling of radiative trap B

C_2 = conversion factor for empty traps

C_4 = conversion factor for filled traps

B_o = original number of traps of type B.

E^* is a scavenger trap which has caught an electron from a radiative trap upon readout. E^* is computed as follows:

$$E^* = E_o \, e^{-C_5 R} \left(1 - e^{-K_3 A^*}\right)$$

where: K_3 = rate of filling of the scavenger trap

C_5 = rate of transformation of scavenger trap

E_o = original number of scavenger traps.

Similarly $F^* = F_o \, e^{-C_6 R} \left(1 - e^{-K_4 B^*}\right)$

where: F_o = original number of scavenger traps

C_6 = rate of transformation of scavenger traps

K_4 = rate of filling of scavenger traps.

For a test of the model against available published data, simplification is justified because the published data does not distinguish between the areas under the individual peaks in the glow curve. The simplification is to assume a single type of radiative trap (A = A + B),

a single type of scavenger trap (E = E + F), and a single type of conversion trap (C = C + D). Empirical fitting of the constants leads to the following response equation:

$$S = 572{,}500\ (e^{-2.6 \times 10^{-7} R} - e^{-2.5 \times 10^{-5} R}) - 9{,}300{,}000\ e^{-9 \times 10^{-6} R}\ (1 - e^{-1 \times 10^{-7} A^*})$$

where: $$A^* = 572{,}500\ (e^{-2.6 \times 10^{-7} R} - e^{-2.5 \times 10^{-5} R})$$

Even with this simplification the model describes the response vs. dose and the sensitivity increase of the dosimeter fairly well. The simplified model fails to accurately account for the damage to the dosimeters; however, by including both types of radiative traps ($A^* + B^*$), it is possible to describe with good accuracy both single-exposure and multiple exposure damage.

Thus it appears that the developed model does give a fairly accurate qualitative picture of the response of the LiF dosimeter. It is thought that further work on the model, in particular, an attempt to separate the two glow curves and obtain a separate evaluation of A^*, B^*, E^* and F^* would greatly enhance the accuracy with which the model predicts the response of the LiF dosimeter.

To extend this problem, it would be necessary to obtain a source of data for each of the two glow peaks under consideration. This might be accomplished by refinement of readout instruments, or by mathematical curve-fitting techniques. If the glow peaks are successfully separated, experiments could be undertaken to determine

the effects of radiation damage and annealing procedure on each individual peak. It is thought that an accurate quantatitive model could then be developed.

BIBLIOGRAPHY

[1] J. R. Cameron, N. Suntharalingam, G. N. Kenney, Thermoluminescent Dosimetry, The University of Wisconsin Press, Madison, Wisconsin (1968), pp. 3-7, 30-45, 131-181.

[2] C. Kittel, Introduction to Solid State Physics, third edition, John Wiley & Sons, Inc., New York, New York (1967), pp. 1-33, 559-615.

[3] Amperex Electronic Corporation, "Thermoluminescent Dosimetry," advance edition, (1967).

[4] S. Glasstone and A. Sesonske, Nuclear Reactor Engineering, 2nd ed., D. Van Nostrand Co., Inc., Princeton, New Jersey (1963), p. 49-50.

[5] Robley D. Evans, The Atomic Nucleus, McGraw-Hill Book Company, Inc., New York, New York (1955), pp. 684-690.

[6] Randall, J. T., and Wilkins, M. H. F., Phospherescence and Electron Traps., Proc. Royal Society (A) 184, (1945).

[7] Ballard, William Wade, Jr., "The Damage Effects of High Energy Radiation on Lithium Fluoride Thermoluminescent Dosimeters." a thesis at Louisiana State University, August, 1968.

VITA

Joseph David Bankston, Jr. was born in New Orleans, Louisiana, on July 2, 1945. He received his secondary education at Ponchatoula High School in Ponchatoula, Louisiana, from which he graduated in April, 1963. In September of that year he enrolled in Louisiana State University, Baton Rouge, Louisiana. The Bachelor of Science Degree in Mechanical Engineering was granted to him in August, 1967. Upon graduation he enrolled in the Graduate School of Louisiana State University and is now a candidate for the Master of Science Degree in Nuclear Engineering in January, 1969.